Pharm Res (2015) 32:1676–1693
DOI 10.1007/s11095-014-1566-1

RESEARCH PAPER

Synthesis and Evaluation of Anticancer Activity in Cells of Novel Stoichiometric Pegylated Fullerene-Doxorubicin Conjugates

George E. Magoulas • Marina Bantzi • Danai Messari • Efstathia Voulgari • Chrisostomi Gialeli • Despoina Barbouri • Athanassios Giannis • Nikos K. Karamanos • Dionissios Papaioannou • Konstantinos Avgoustakis

Received: 1 July 2014 / Accepted: 29 October 2014 / Published online: 8 November 2014

ABSTRACT

Purpose To synthesize pegylated stoichiometrically and structurally well-defined conjugates of fullerene (C_{60}) with doxorubicin (DOX) and investigate their antiproliferative effect against cancer cell lines.

Methods Stoichiometric (1:1 and 1:2) pegylated conjugates of C_{60} with DOX were synthesized using the Prato reaction to create fulleropyrrolidines equipped with a carboxyl function for anchoring a polyethylene glycol (PEG) moiety and either a hydroxyl group for attaching one molecule of DOX or a terminal alkyne group for attaching two molecules of DOX through a click reaction. In both conjugates, the DOX moieties are held through a urethane-type bond. Drug release was studied in phosphate buffer (PBS, pH 7.4) and MCF-7 cancer cells lysate. The uptake of the conjugates by MCF-7 cancer cells and their intracellular localization were studied with fluorescence microscopy. The antiproliferative activity of the conjugates was investigated using the WST-1 test.

Results One or two DOX molecules were anchored on pegylated C_{60} particles to form DOX-C_{60}-PEG conjugates. Drug liberation from the conjugates was significantly accelerated in the presence of tumor cell lysate compared to PBS. The conjugates could be internalized by MCF-7 cells. DOX from the conjugates exhibited much delayed, compared to free DOX, localization in the nucleus and antiproliferative activity.

Conclusion Pegylated DOX-C_{60} conjugates (1:1) and (2:1) with well-defined structure were successfully synthesized and found to exhibit comparable, but with a delayed onset, antiproliferative activity with free DOX against MCF-7 cancer cells. The results obtained justify further investigation of the potential of these conjugates as anticancer nanomedicines.

KEY WORDS antiproliferative activity · conjugates · doxorubicin · fullerenes · nanoparticles

ABBREVIATIONS

DIAD	diisopropyl azodicarboxylate
DIC	*N,N′*-diisopropylcarbodiimide
FCC	Flash Column Chromatography
HBTU	*O*-(benzotriazol-1-yl)-*N,N,N′,N′*-tetramethyluronium hexafluorophosphate
HOSu	*N*-hydroxysuccinimide
MeO-PEG-NH_2	amino-polyethylene glycol monomethyl ether

INTRODUCTION

Since their discovery in 1985 by Kroto *et al.* (1) fullerenes (e.g. C_{60}, **I**) have attracted considerable interest in many fields of research, including material science and biomedicine. Pristine fullerene is insoluble in water. Covalent attachment of various groups (e.g., −OH, $-NH_2$, −COOH) to the fullerene cage

Electronic supplementary material The online version of this article (doi:10.1007/s11095-014-1566-1) contains supplementary material, which is available to authorized users.

G. E. Magoulas • D. Papaioannou
Laboratory of Synthetic Organic Chemistry, Department of Chemistry University of Patras, 26504 Patras, Greece

M. Bantzi • D. Messari • E. Voulgari • K. Avgoustakis (✉)
Department of Pharmacy University of Patras, 26504 Patras, Greece
e-mail: avgoust@upatras.gr

C. Gialeli • D. Barbouri • N. K. Karamanos
Laboratory of Biochemistry, Department of Chemistry University of Patras, 26504 Patras, Greece

A. Giannis
Institut für Organische Chemie, Fakultät für Chemie und Mineralogie Universität Leipzig, Johannisallee 29, 04103 Leipzig, Germany

results in the formation of "functionalized" fullerene particles with increased aqueous solubility, which can be used for biomedical applications (2). Fullerenes are attractive candidates for drug delivery applications because they exhibit certain superior characteristics compared to available, widely used nanocarriers (such as liposomes, polymeric nanoparticles and dendrimers). Thus, fullerenes have a well-defined shape (their spherical shape is unequalled in nature) and particle size, and large surface area (due to their very small size of 7–10 Å). Their unique chemical structure allows for controlled synthetic modifications in order to obtain fullerene derivatives with tailor-made properties (2,3). Furthermore, fullerenes are biologically stable and their convenient three-dimensional scaffolding allows for covalent attachment of drug molecules. Functionalized fullerenes have been investigated for the delivery of therapeutic agents (4) and radioisotopes (5) as well as genes (6), and imaging agents (7). The application of fullerenes as carriers of chemotherapeutics in particular, is still in a very nascent stage (8). There are only a few reports in the literature where fullerene derivatives have been proposed for the delivery of chemotherapeutics, such as doxorubicin (DOX) (8–10) and paclitaxel (11,12).

Attachment of other structural units or drugs on C_{60} is possible only following its derivatization through a variety of reactions, most often the Prato reaction, the Bingel-Hirsch reaction or the Diels-Alder reaction (13). Derivatization not only secures the presence of one or more handles for anchoring the desired molecules, but also leads to a substantial improvement of the solubility of C_{60} in organic solvents, thus facilitating subsequent reactions on the functionalized fullerene. We are interested in the development of stoichiometrically and structurally well-defined fullerene constructs (Fig. 1), which could deliver one or two same, e.g. DOX (**2**), or different anticancer agents, incorporating at the same time water solubility enhancing structural motifs, e.g. polyethylene glycol units. In this work, we report our results on the synthesis of the pegylated DOX-C_{60} conjugates **7a**, **7b** and **8** (Fig. 1), using the fullerenopyrrolidine constructs **6a-c** as key-intermediates, and their evaluation as potential antiproliferative agents/prodrugs. In these conjugates, anchoring of the anticancer drug(s) on the construct was effected through urethane bond whereas the water solubility enhancer polyethylene glycol (PEG) was incorporated through an amide bond. Although, as mentioned above DOX-C_{60} conjugates have already been reported in the literature, the conjugates synthesized were either non-stoichiometric and not well-defined structurally, such as in the case of "fullerenols" (8), or the drug was attached to fullerene nanoparticles through a hydrolytically stable amide bond (9,10), limiting their potential applications as drug delivery systems.

MATERIALS AND METHODS

Materials

Fullerene (C_{60}) and doxorubicin hydrochloride were purchased from SES research (USA) and LC laboratories (USA), respectively. MeO-PEG-NH_2 at a molecular weight of 2,000 was purchased from Laysan Bio, Inc. All other chemicals and reagents used were at least of analytical grade.

Chemistry

Capillary melting points were taken on a Büchi SMP-20 apparatus and are uncorrected. IR spectra were recorded as KBr pellets, unless otherwise stated, on a Perkin-Elmer 16PC FT-IR spectrophotometer. UV/Vis spectra were obtained on a Varian Cary 50 spectrometer using UV 10 mm quartz suprasil cells from Hellma. ^{1}H-NMR spectra were obtained at 400.13 MHz and ^{13}C-NMR at 100.62 MHz on a Bruker Avance 400 DPX spectrometer. Electron-Spray Ionization (ESI) mass spectra were obtained on a Micromass-Platform LC spectrometer for solutions of the measured compounds in MeOH. Thermogravimetric analysis (TGA) was carried out on ~5 mg samples contained in alumina crucibles in a Labsys TM TG apparatus of Setaram under nitrogen and at a heating rate of 10°C/min up to 700°C. Flash Column Chromatography (FCC) was performed on Merck silica gel 60 (230–400 mesh) and Thin Layer Chromatography (TLC) on Merck silica gel F_{254} films (0.2 mm) precoated on aluminium foil. Spots were visualized with UV light at 254 nm. All solvents used were dried according to standard procedures prior to use. Experiments were routinely conducted under an atmosphere of Ar and with protection from light. Drying of solutions was effected with anhydrous Na_2SO_4, whereas evaporation of the solvents was performed under reduced pressure in a rotary evaporator at a bath temperature not exceeding 40°C. Fullerene (C_{60}) and doxorubicin hydrochloride were purchased from SES research (USA) and LC laboratories (USA), respectively. MeO-PEG-NH_2 at a molecular weight of 2,000 was purchased from Laysan Bio, Inc. The *N*-alkylated glycine derivative **9** (Scheme 1) was prepared according to the procedure described in ref. 13. The preparation and full characterization of key-intermediates **11**, **12**, **14**, **15** (Scheme 1) and **23**–**25** (Scheme 3) can be found in supporting information.

General Procedure for the Prato Reaction Between C_{60}, Isovanillin Derivatives 11 or 12 and N-alkylated Glycine 9 or 15

A solution of C_{60} (0.16 g, 0.22 mmol), aldehyde **11** or **12** (0.66 mmol) and glycine (Gly) derivative **9** or **15** (0.22 mmol) in PhMe (70 ml) was heated to reflux for 4 h. Then, the

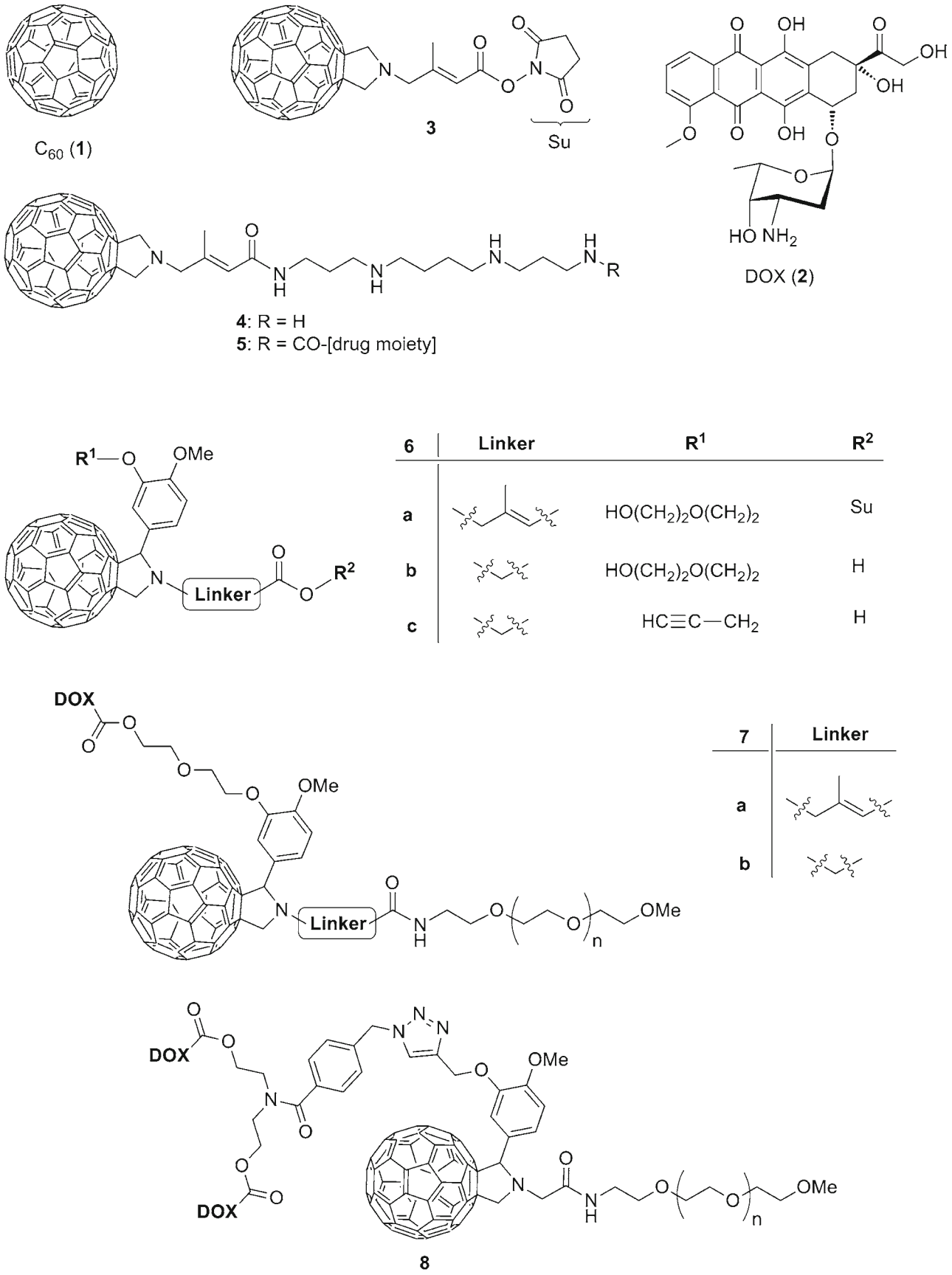

Fig. 1 Lead and designed compounds.

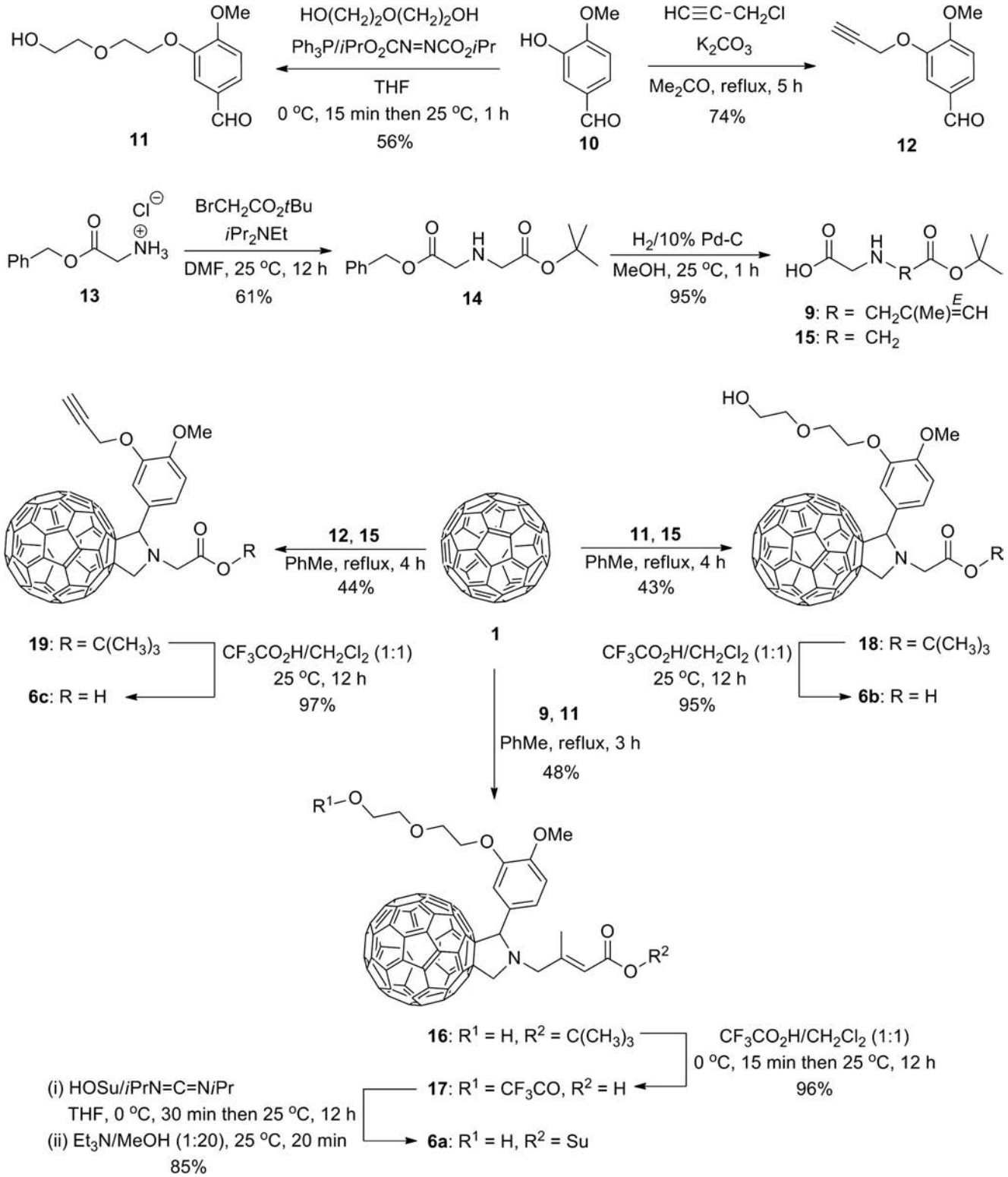

Scheme 1 Synthesis of the fullerenopyrrolidine derivatives **6a-c**.

reaction mixture was left to attain ambient temperature, evaporated under vacuo to a minimum volume and was subsequently subjected to FCC using PhMe as eluent. Unreacted C_{60} was first recovered and then the appropriate elution solvent (see below) was applied to afford compounds **16**, **18** or **19**. The calculated yields of the Prato reaction adducts are based on the initial quantity of C_{60} used.

Fullerenopyrrolidine Derivative 16

Yield: 0.12 g (48%); brown solid; R_f (PhMe/EtOAc 1:1 *v/v*): 0.4; IR (KBr, cm^{-1}): 3492, 2918, 1702, 1646, 1594, 1260, 1232, 1136, 1024, 862, 804, 728; MS (ESI, 30 eV): *m/z* 1166.08 (M+K), 1150.46 (M+Na); ^{1}H NMR ($CDCl_3$): δ 7.12-7.06 (2H, m), 6.84 (1H, d, J=8.0 Hz), 6.13 (1H, s), 5.04 (1H, s), 4.88 (1H, d, J=9.6 Hz), 4.14-4.07 (2H, m), 4.02 (1H, d, J=9.6 Hz), 3.90 (1H, d, J=14.0 Hz), 3.82-3.78 (2H, m), 3.79 (3H, s), 3.69-3.65 (2H, m), 3.59-3.56 (2H, m), 3.00 (1H, d, J=14.0 Hz), 2.28 (3H, s), 1.48 (9H, s); ^{13}C NMR ($CDCl_3$): δ 165.9, 153.4, 152.9, 150.0, 147.4, 146.6, 146.4, 146.3, 146.2, 146.1, 146.0, 145.8, 145.6, 145.4, 145.3, 145.2, 144.8, 144.6, 144.4, 144.3, 143.2, 143.0, 142.7, 142.6, 142.3, 142.2, 142.0, 141.9, 141.7, 141.5, 140.2, 140.1, 139.9, 139.7, 129.0 (two C), 128.2 (two C), 125.3, 81.6, 72.6, 69.1, 68.6, 68.3, 61.7, 61.1, 55.8, 27.3 (three C), 21.5.

Fullerenopyrrolidine Derivative 18

Yield: 0.10 g (43%); brown solid; R_f (PhMe/EtOAc 1:1 *v/v*): 0.21; IR (KBr, cm^{-1}): 3406, 2916, 1698, 1646, 1504, 1430, 1354, 1246, 1130, 1030, 862, 806, 726; MS (ESI, 30 eV): *m/z* 1126.42 [M+K], 1110.11 [M+Na], 1088.15 [M+H]; ^{1}H NMR ($CDCl_3$): δ 7.19-7.13 (m, 2H), 6.92 (d, J=8.0 Hz, 1H), 5.46 (s, 1H), 5.20 (d, J=9.2 Hz, 1H), 4.57 (d, J=9.2 Hz, 1H), 4.20-4.15 (m, 2H), 3.99 (d, J=16.4 Hz, 1H), 3.92-3.88 (m, 2H), 3.86 (s, 3H), 3.76-3.73 (m, 2H), 3.69-3.65 (m, 2H), 3.53 (d, J=16.4 Hz, 1H), 1.58 (s, 9H); ^{13}C NMR ($CDCl_3$): δ 169.6, 154.0, 153.6, 153.5, 148.4, 146.8, 146.4, 146.3, 146.2, 146.1, 146.0, 145.9, 145.8, 145.7, 145.6, 145.4, 145.3, 145.2, 145.1, 145.0, 144.8, 144.6, 144.4, 144.3, 143.2, 142.9, 142.6, 142.3, 142.2, 142.1, 142.0, 141.8, 141.7, 141.6, 140.2, 140.1, 139.8, 139.6, 136.7, 136.6, 135.8, 135.7,129.3,129.0, 128.2, 125.3, 112.9, 81.7, 79.7, 72.6, 69.4, 68.8, 68.3, 66.0, 61.7, 56.1, 28.3 (three C).

Fullerenopyrrolidine Derivative 19

Yield: 0.10 g (44%); brown solid; R_f (PhMe): 0.20; IR (KBr, cm^{-1}): 3442, 3299, 2916, 2852, 2116, 1728, 1642, 1506, 1440, 1372, 1260, 1140, 1026, 804; MS (ESI, 30 eV): *m/z* 1076.66 [M+K], 1060.80 [M+Na], 1038.12 [M+H]; ^{1}H NMR ($CDCl_3$): δ 7.64-7.47 (m, 1H), 7.44-7.32 (m, 1H), 6.93 (d, J=8.4 Hz, 1H), 5.47 (s, 1H), 5.20 (d, J=9.2 Hz, 1H), 4.78 (d, J=2.4 Hz, 2H), 4.56 (d, J=9.2 Hz, 1H), 4.00 (d, J=16.8 Hz, 1H), 3.88 (s, 3H), 3.54 (d, J=16.8 Hz, 1H), 2.42 (unresolved t, 1H), 1.58 (s, 9H); ^{13}C NMR ($CDCl_3$): δ 169.5, 156.3, 154.0, 153.5, 149.9, 147.3, 146.8, 146.5, 146.2, 146.0, 145.9, 145.8, 145.5, 145.4, 145.3, 145.2, 145.1, 144.7, 144.6, 144.4, 144.3, 143.1, 143.0, 142.7, 142.6, 142.5, 142.3, 142.2, 142.1, 142.0, 141.9, 141.8, 141.6, 141.5, 140.2, 139.8, 139.6, 137.0, 136.6, 135.9, 135.7, 129.0, 128.5, 128.2, 125.3, 123.7, 111.5, 81.6, 79.5, 78.4, 76.3, 65.9, 56.7, 55.8, 53.0, 28.3 (three C).

General Procedure for the Cleavage of the Tert-butyl Ester Group from Prato Adducts 16, 18 or 19

To a solution of *tert*-butyl ester **16**, **18** or **19** (0.083 mmol) in CH_2Cl_2 (1 ml), TFA (1 ml) was added and the mixture was stirred at ambient temperature for 2 h (16 h in the case of ester **16**). Then, the reaction mixture was evaporated to dryness and triturated with hexane. Acids **6b**, **6c** and **17** were obtained upon filtration.

Fullerenopyrrolidine Acid 6b

Yield: 0.081 g (95%); brown solid; R_f (PhMe/EtOAc 3:7 *v/v*): 0.22; IR (KBr, cm^{-1}): 3428, 2922, 1720, 1666, 1510, 1452, 1424, 1262, 1174, 1142, 1048, 756; MS (ESI, 30 eV): *m/z* 1054.10 [M+Na], 1032.20 [M+H].

Fullerenopyrrolidine Acid 6c

Yield: 0.079 g (97%); brown solid; R_f (PhMe/EtOAc 8:2 *v/v*): 0.20; IR (KBr, cm^{-1}): 3440, 3296, 2922, 2850, 2122, 1722, 1648, 1512, 1438, 1262, 1180, 1146, 1022; MS (ESI, 30 eV): *m/z* 1020.31 [M+K], 982.03 [M+H].

O-Trifluoroacetylated Fullerenopyrrolidine Acid 17

Yield: 0.093 g (96%); brown solid; R_f (PhMe/EtOAc 1:1 *v/v*): 0.20; MS (ESI, 30 eV): *m/z* 1206.12 (M+K), 1190.19 (M+Na), 1168.02 (M+H).

Fullerenopyrrolidine Succinimidyl Ester 6a

To an ice-cold solution of **17** (0.065 g, 0.06 mmol) in THF (0.3 ml), HOSu (0.021 g, 0.18 mmol) and DIC (19 µl, 0.12 mmol) were added sequentially. The reaction mixture was stirred at 0°C for 30 min and then overnight at ambient temperature. It was then diluted with $CHCl_3$, washed twice with an aqueous solution of 5% $NaHCO_3$ and twice with water. The organic layer was dried over Na_2SO_4 and then evaporated to dryness. The residue was treated with Et_3N (100 µl) in MeOH (2 ml) for 20 min in order to cleave the trifluoroacetyl moiety. The resulting mixture was re-evaporated to dryness and subjected to FCC to afford pure succinimidyl ester **6a**.

Yield: 0.06 g (85%); brown solid; R_f (PhMe/EtOAc 1:1 *v/v*): 0.10; IR (KBr, cm^{-1}): 3486, 2924, 1735, 1646, 1542; MS (ESI, 30 eV): *m/z* 1207.13 (M+K), 1191.14 (M+Na), 1169.11 (M+H); ^{1}H NMR ($CDCl_3$): δ 7.19-7.13 (2H, m), 6.92 (1H, d, J=8.0 Hz), 6.80 (1H, s), 5.20 (1H, s), 5.02 (1H, d, J=9.6 Hz), 4.22-4.16 (2H, m), 4.14 (1H, d, J=9.6 Hz), 4.06

(1H, d, $\mathcal{J}$=16.6 Hz), 3.90-3.83 (2H, m), 3.86 (3H, s), 3.75-3.71 (2H, m), 3.67-3.63 (2H, m), 3.27 (1H, d, $\mathcal{J}$=16.6 Hz), 2.88 (4H, br. s), 2.47 (3H, s); ^{13}C NMR ($CDCl_3$): δ 165.8 (three C), 153.2, 152.8, 150.1, 147.3, 146.6, 146.4, 146.3, 146.2, 146.1, 146.0, 145.7, 145.6, 145.4, 145.3, 145.2, 144.8, 144.6, 144.4, 144.3, 143.2, 142.9, 142.7, 142.6, 142.3, 142.2, 142.0, 141.9, 141.7, 141.4, 140.2, 140.1, 139.9, 139.7, 129.3 (two C), 128.5 (two C), 125.4, 81.2, 72.4, 69.5, 68.9, 68.3, 61.2, 60.9, 55.7, 25.6 (two C), 21.4.

General Procedure for the Preparation of the C_{60}-PEG Constructs 20b and 26

To an ice-cold suspension of **6b** or **6c** (0.048 mmol) in $CHCl_3$ (0.2 ml), MeO-PEG-NH_2 (MW=2000) (0.106 g, 0.053 mmol), Et_3N (20 µl, 0.144 mmol) and HBTU (0.022 g, 0.058 mmol) were added sequentially. The resulting mixture was stirred at ambient temperature overnight and then evaporated to dryness. The residue was subjected to FCC to provide constructs **20b** and **26**, respectively, as brown oils which were solidified upon treatment with Et_2O.

C_{60}-PEG Construct 20b

Yield: 0.09 g (62%); brown solid; R_f ($CHCl_3$/MeOH 95:5 *v/v*): 0.15; IR (KBr, cm^{-1}): 3424, 2876, 1654, 1514, 1466, 1344, 1242, 1108, 952, 842; ^{1}H NMR ($CDCl_3$): δ 7.93 (t, $\mathcal{J}$= 4.8 Hz, 1H), 7.30-7.26 (m, 2H), 6.93 (d, $\mathcal{J}$=8.0 Hz, 1H),5.28 (s, 1H),5.06 (d, $\mathcal{J}$=9.6 Hz, 1H), 4.32 (d, $\mathcal{J}$=9.6 Hz, 1H), 4.19-4.13 (m, 2H), 3.97 (d, $\mathcal{J}$=16.0 Hz, 1H), 3.83 (s, 3H), 3.81-3.77 (m, 2H), 3.74-3.70 (m, 6H), 3.67-3.55 (br. s, MeO-PEG main chain), 3.55-3.51 (m, 4H), 3.48-3.43 (m, 2H), 3.37 (s, 3H).

C_{60}-PEG Construct 26

Yield: 0.088 g (62%); brown solid; R_f ($CHCl_3$/MeOH 95:5 *v/v*): 0.15; IR (KBr, cm^{-1}): 3446, 2874, 1668, 1514, 1464, 1344, 1254, 1106, 952, 842; ^{1}H NMR ($CDCl_3$): δ 7.95 (t, $\mathcal{J}$= 4.8 Hz, 1H), 7.53-7.47 (m, 1H), 7.34 (d, $\mathcal{J}$=8.0 Hz, 1H), 6.93 (d, $\mathcal{J}$=8.0 Hz, 1H), 5.32 (s, 1H), 5.07 (d, $\mathcal{J}$=9.6 Hz, 1H), 4.77-4.75 (m, 2H), 4.33 (d, $\mathcal{J}$ =9.6 Hz, 1H), 4.00 (d, $\mathcal{J}$=16.4 Hz, 1H), 3.87 (s, 3H), 3.83-3.76 (m, 2H), 3.75-3.69 (m, 2H), 3.67-3.56 (br. s, MeO-PEG main chain), 3.56-3.51 (m, 4H), 3.37 (s, 3H), 2.51-2.48 (m, 1H).

C_{60}-PEG Construct 20a

To an ice-cold solution of **6a** (0.035 g, 0.041 mmol) in $CHCl_3$ (0.13 ml), Et_3N (9 µl, 0.062 mmol) and MeO-PEG-NH_2 (MW=2000) (0.090 g, 0.045 mmol) were added sequentially. The resulting mixture was stirred at ambient temperature for 1 h and then evaporated to dryness. The residue was subjected to FCC to give construct **20a** as a brown oil which was solidified upon treatment with Et_2O.

Yield: 0.117 g (94%); brown solid; R_f ($CHCl_3$/MeOH 9:1 *v/v*): 0.4; IR (KBr, cm^{-1}): 3440, 2886, 1636, 1344, 1114; ^{1}H NMR ($CDCl_3$): δ 7.23-7.12 (2H, m), 6.92 (1H, d, $\mathcal{J}$=8.4 Hz), 6.48 (1H, br.s), 6.25 (1H, s), 5.09 (1H, s), 4.95 (1H, d, $\mathcal{J}$=9.4 Hz), 4.19-4.14 (2H, m), 4.05 (1H, d, $\mathcal{J}$=9.4 Hz), 3.95 (1H, d, $\mathcal{J}$= 16 Hz), 3.90-3.83 (2H, m), 3.85 (3H, s), 3.81-3.78 (2H, m), 3.75-3.70 (2H, m), 3.69-3.66 (2H, m), 3.66-3.54 (br. s, MeO-PEG main chain), 3.59-3.55 (4H, m), 3.47-3.42 (2H, m), 3.36 (3H, s), 3.02 (1H, d, $\mathcal{J}$=16 Hz), 2.50 (3H, s).

General Procedure for the Activation of the Hydroxyl Function of C_{60}-PEG Constructs with p-nitrophenyl Chloroformate

To a solution of **20a** or **20b** (0.027 mmol) in THF (0.14 ml), Et_3N (9 µl, 0.0675 mmol) and *p*-nitrophenyl chloroformate (0.011 g, 0.054 mmol) were added with that order. The reaction mixture was stirred at ambient temperature for 12 h and then subjected to FCC to provide activated constructs **21a** or **21b**, respectively, as brown solids upon treatment with Et_2O.

Activated C_{60}-PEG Construct 21a

Yield: 0.072 g (83%); brown solid; R_f ($CHCl_3$/MeOH 95:5 *v/v*): 0.2; IR (KBr, cm^{-1}): 3511, 2872, 1768, 1669, 1522, 1459, 1349, 1253, 1106, 947, 851; ^{1}H NMR ($CDCl_3$): δ 8.24 (2H, d, $\mathcal{J}$=8.8 Hz), 7.35 (2H, d, $\mathcal{J}$=8.8 Hz), 6.97-6.90 (2H, m), 6.36 (1H, m), 6.21 (1H, s), 5.08 (1H, s), 4.94 (1H, d, $\mathcal{J}$=9.6 Hz), 4.46-4.40 (2H, m), 4.22-4.15 (2H, m), 4.05 (1H, d, $\mathcal{J}$=9.6 Hz), 3.99-3.88 (3H, m), 3.85 (3H, s), 3.82-3.79 (2H, m), 3.67-3.55 (br.s, MeO-PEG main chain), 3.48-3.43 (2H, m), 3.37 (3H, s), 3.01 (1H, d, $\mathcal{J}$=9.6 Hz), 2.52 (3H, s).

Activated C_{60}-PEG Construct 21b

Yield: 0.069 g (80%); brown solid; R_f ($CHCl_3$/MeOH 95:5 *v/v*): 0.15; IR (KBr, cm^{-1}): 3504, 2875, 1770, 1674, 1467, 1352, 1256, 1106, 953; ^{1}H NMR ($CDCl_3$): δ 8.24 (d, $\mathcal{J}$= 8.8 Hz, 2H), 7.94 (t, $\mathcal{J}$=4.8 Hz, 1H), 7.35 (d, $\mathcal{J}$=8.8 Hz, 2H), 7.29-7.24 (m, 2H), 6.94 (d, $\mathcal{J}$=8.0 Hz, 1H), 5.28 (s, 1H), 5.05 (d, $\mathcal{J}$=9.6 Hz, 1H), 4.46-4.39 (m, 2H), 4.31 (d, $\mathcal{J}$=9.6 Hz, 1H), 4.21-4.15 (m, 2H), 3.98 (d, $\mathcal{J}$=16.0 Hz, 1H), 3.94-3.90 (m, 2H), 3.89-3.84 (m, 2H), 3.82 (s, 3H), 3.81-3.78 (m, 2H), 3.67-3.55 (br.s, MeO-PEG main chain), 3.47-3.42 (m, 2H), 3.36 (s, 3H), 3.33 (d, $\mathcal{J}$=16.0 Hz, 1H).

General Procedure for Coupling Activated C_{60}-PEG Constructs 21a or 21b with Doxorubicin Hydrochloride

A solution of construct **21a** or **21b** (0.02 mmol) in DMF (0.25 ml) was added to a solution of doxorubicin hydrochloride (0.012 g, 0.02 mmol) and Et_3N (4 μl) in DMF (0.9 ml). The resulting mixture was stirred at ambient temperature overnight and evaporated under high vacuo. Purification with FCC followed by trituration with Et_2O yielded conjugate **7**.

DOX-C_{60}-PEG Conjugate 7a

Yield: 0.061 g (84%); red solid; R_f ($CHCl_3$/MeOH 95:5 *v/v*): 0.22; IR (KBr, cm^{-1}): 3450, 2905, 1725, 1635, 1612, 1454, 1352, 1276, 1246, 1110, 950, 844.

DOX-C_{60}-PEG Conjugate 7b

Yield: 0.047 g (65%); red solid; R_f ($CHCl_3$/MeOH 9:1 *v/v*): 0.19; IR (KBr, cm^{-1}): 3444, 2906, 1714, 1644, 1616, 1454, 1352, 1286, 1252, 1108, 952, 846.

Click Reaction Between Azide 25 and C_{60}-PEG Construct 26

To a solution of azide **25** (0.056 g, 0.09 mmol) and terminal alkyne **26** (0.093 g, 0.03 mmol) in DCM/H_2O (1:1, 1.8 ml), $CuSO_4 \cdot 5H_2O$ (1.1 mg) and sodium ascorbate (1.4 mg) were added. The reaction mixture was stirred vigorously at ambient temperature for 24 h. Then, it was evaporated to dryness and subjected to FCC to afford the doubly activated C_{60}-PEG construct **27** which solidified upon treatment with Et_2O.

Yield: 0.076 g (71%); brown solid; R_f ($CHCl_3$/MeOH 92:8 *v/v*): 0.15; IR (KBr, cm^{-1}): 3490, 2888, 1761, 1648, 1620, 1535, 1351, 1107, 955, 871; ^{1}H NMR ($CDCl_3$): δ 8.26 (d, $\mathcal{J}$= 8.8 Hz, 4H), 8.10 (unresolved t, 1H), 7.58 (s, 1H), 7.43 (d, $\mathcal{J}$= 8.0 Hz, 2H), 7.40-7.31 (m, 4H), 7.28 (d, $\mathcal{J}$=8.0 Hz, 2H), 7.27-7.25 (m, 2H), 6.92 (d, $\mathcal{J}$=9.2 Hz, 1H), 5.50 (s, 1H), 5.28 (s, 2H), 5.09 (d, $\mathcal{J}$=9.2 Hz, 1H), 4.64-4.52 (m, 2H), 4.39-4.28 (m, 2H), 4.31 (d, $\mathcal{J}$=9.2 Hz, 1H), 4.00-3.92 (m, 2H), 3.98 (d, $\mathcal{J}$= 16.0 Hz, 1H), 3.84 (s, 3H), 3.82-3.78 (m, 2H), 3.76-3.71 (m, 4H), 3.67-3.60 (br. s, MeO-PEG main chain), 3.48-3.44 (m, 2H), 3.37 (s, 3H), 3.34 (d, $\mathcal{J}$=16.0 Hz, 1H).

DOX-C_{60}-PEG Conjugate 8

A solution of construct **27** (0.053 g, 0.015 mmol) in DMF (0.20 ml) was added to a solution of doxorubicin hydrochloride (0.017 g, 0.03 mmol) and Et_3N (6.0 μl, 0.045 mmol) in DMF (0.7 ml) and the resulting mixture was stirred at ambient temperature overnight. Then, it was evaporated under high vacuo and subjected to FCC. The residue was precipitated upon treatment with Et_2O and dried to give conjugate **8**.

Yield: 0.043 g (66%); red solid; R_f ($CHCl_3$/MeOH 9:1 *v/v*): 0.10; IR (KBr, cm^{-1}): 3442, 2972, 2868, 1716, 1616, 1576, 1444, 1286, 1108, 1018, 986, 948, 808.

Physicochemical Characterizations and Drug Release from Conjugates

The aqueous solubility of synthesized conjugates was evaluated at 20°C. Dissolution was facilitated by sonication.

The particle size (average and distribution) of conjugates dispersions in distilled water were determined by dynamic light scattering (DLS) in a Malvern Nano-ZS zetasizer.

Drug release from conjugates was studied in phosphate buffered saline pH 7.4 (PBS) and tumor cell lysate. Tumor cell lysate was obtained from MCF-7 cells (10^6 cells) using the M-PER protein extraction reagent (PIERCE) and following the instructions of the manufacturer. Pegylated DOX-C_{60} particles (conjugate **8**) were suspended in tumor cell lysate or PBS at a concentration of 100 μg/ml, enclosed in dialysis bags (Spectrapor, molecular weight cutoff 2000) and dialyzed against 10 ml PBS in a mildly shaking water bath (37°C). At predetermined time intervals, the release medium was replaced by fresh PBS (37°C), and the release medium containing the liberated drug (DOX) was assayed for drug by absorption spectroscopy at 485 nm.

Biological Evaluation

Cell Culture

Breast cancer cells of human breast adenocarcinoma, MCF-7 (ATCC® HTB-22) were obtained from the American Tissue Culture Collection. Breast cancer cells were cultured in DMEM supplemented with 10% (*v/v*) FBS, 1.0 mM sodium pyruvate, and a cocktail of antimicrobial agents (100 IU/mL penicillin, 100 μg/mL streptomycin, 10 μg/mL gentamicin sulfate, 10 μg/mL L-glutamine and 2.5 μg/mL amphotericin B). Cells were routinely grown at 37°C in a humidified atmosphere of 5% (*v/v*) CO_2. Culture medium was changed every 48 h. Cells were harvested by trypsinization with 0.05% (*w/v*) trypsin in PBS containing 0.02% (*w/v*) Na_2EDTA.

Cell Proliferation Assay

In order to evaluate the effects of the compounds on breast cancer cell proliferation, cells were seeded in the presence of serum into 96-well plates at a density of 8,000 cells/well. Twenty-four h after plating, new medium supplemented with the compounds, was added in different concentrations: 0.01 μM, 0.05 μM, 0.15 μM, 0.5 μM, 1.5 μM, 10 μM, 20 μM. All stock materials were diluted in 1.5% (*v/v*) DMSO (dimethyl sulfoxide) in water. In all incubations DMSO concentration was maintained at 0.1% (*v/v*) in order to ascertain

solubility of the materials. After 48 h or 72 h incubation, fresh medium was added in order to prevent any potential intervention of DOX in the assay and WST-1 (water-soluble tetrazolium salt) was added at a ratio 1:10. The assay is based on the reduction of WST-1 by viable cells, producing a soluble formazan salt and its absorbance is measured at 450 nm (reference wavelength at 650 nm) (14). The IC_{50} values for DOX and DOX conjugates are calculated by the dose–response curve fit using Graph Pad Prism 6.0.

Cellular Uptake Studies

MCF7 cells were seeded on glass coverslips in 24-well plates and grown to 80% confluence prior to treatment. The materials were added to the cells in DMEM serum free medium containing 0.1% (*v*/*v*) DMSO at 10 μM. In different time points (15 min, 30 min, 1, 24, 48 and 72 h) cells were washed once with PBS buffer, fixed with 4% formaldehyde in PBS buffer for 20 min at room temperature, then washed three times with PBS-Tween buffer and mounted on glass slides using mounting buffer with DAPI (Invitrogen). Images were obtained using Olympus inverted fluorescence microscope (×60 magnification). The total DOX located in the cell (free or conjugated) at the different time points was quantified measuring the total fluorescence in each cell at the optical field of each image with Image J, assessing different measurement values such as area, integrated density and mean gray value. The relative fluorescence was measured using the following equation CTCF = Integrated Density – (Area of selected cell x Mean fluorescence of background readings) (15–17).

RESULTS

Synthesis

We have recently shown that polyamines, e.g. spermine, can be efficiently attached (see conjugate **4**, Fig. 1) on a fulleropyrrolidine construct **3** of the α,β-unsaturated 'active' ester type. The latter can selectively acylate primary in the presence of secondary amino functions. Conjugate **4** was further used for the selective attachment of drugs (see conjugate **5**) (18). For the synthesis of compound **3** the Prato reaction of C_{60}, formaldehyde and the Gly derivative **9** (Scheme 1) was used as the key-step. We therefore envisaged that simple replacement of formaldehyde by an easily accessible hydroxy-substituted aromatic aldehyde would provide us the required second arm which could allow us to attach drug molecules. Taking into consideration the fact that urethane bond to a phenol would be more hydrolytically labile than the one to an aliphatic alcohol, we decided to choose isovanillin (**10**), which incorporates a methoxy function in ortho position to the hydroxy group and therefore steric and electronic effect would serve towards stabilizing the urethane bond. However, preliminary experiments showed that activation of the phenolic hydroxyl group as the corresponding p-nitrophenyl carbonate functionality and subsequent aminolysis with the amino group of DOX showed preferential departure of the isovanillin moiety and not the expected 4-nitrophenol. We therefore decided to convert the phenolic hydroxyl group to an aliphatic one by reacting isovanillin with diethylene glycol, under Mitsunobu type reaction conditions. In such wise, the isovanillin derivative **11** was unexceptionally obtained in 56% yield.

Prato reaction between C_{60}, Gly derivative **9** and aldehyde **11** provided the anticipated adduct **16** in 48% yield. CF_3CO_2H-mediated deprotection of *tert*-butyl ester **16** led unexpectedly to simultaneous trifluoroacetylation of the free aliphatic hydroxyl group, thus providing intermediate **17** in 96% yield. Formation of this intermediate could not be avoided neither by using a $CF_3CO_2H/CH_2Cl_2/H_2O$ (1:1:0.2) system nor by inclusion of anisole as a scavenger in the deprotection medium. However, compound **17** was used as such in the next step, namely in the activation of the carboxyl function with HOSu in the presence of DIC. The thus obtained 'active' ester, without purification, was subsequently subjected to selective hydrolysis using a solution of Et_3N in methanol to provide pure 'active' ester **6a** in 85% yield (Scheme 1). Coupling of this ester with MeO-PEG-NH_2, with a mean molecular weight of 2,000, gave the anticipated amide **20a** (Scheme 2) in 94% yield. The free hydroxyl group of this compound was activated through reaction with 4-nitrophenyl chloroformate to afford the expected carbonate mixed ester **21a** in 83% yield, which was then aminolyzed with DOX providing the projected pegylated DOX-C_{60} conjugate **7a** in 84% yield. Detailed structures of conjugates **7a**, **7b** and **8** can be found in supporting information.

Preliminary biological evaluation of **7a** using MCF-7 breast cancer cells revealed that this conjugate presented comparable toxicity to DOX after 48 h incubation (data not shown). Prompted by these results, we decided to simplify the assembly of pegylated DOX-C_{60} conjugates, as concerns the preparation of the N-alkylated Gly derivative required in the Prato reaction, as well as to develop constructs suitable for carrying more than one DOX molecules. Indeed, the initially used Gly derivative **9**, whose synthesis is a multi-step one involving chromatographic purification of intermediates (see ref. 13), was replaced by compound **15** (Scheme 1), which is readily obtained using a two-step protocol. This involved N-alkylation of Gly benzyl ester hydrochloride (**13**) by *tert*-butyl bromoacetate, followed by selective deprotection of the benzyl ester of the so obtained intermediate diester **14** by hydrogenolysis. That way, compound **15** was received in 58% total yield. Prato reaction between C_{60}, isovanilllin

derivative **11** and Gly derivative **15** proceeded unexceptionally, offering the anticipated adduct **18** in 43% yield. CF_3CO_2H-mediated deprotection of the *tert*-butyl ester of adduct **18** gave free acid **6b** (Scheme 1) in 95% yield. This acid was then coupled with MeO-PEG-NH_2 in the presence of the coupling agent HBTU to give amide **20b** (Scheme 2) in 62% yield. This intermediate was then activated with 4-nitrophenyl chloroformate to give the mixed carbonate ester **21b** in 80% yield, which in turn was aminolyzed with DOX giving the pegylated DOX-C_{60} conjugate **7b** in 65% yield.

Incorporation of two molecules of DOX in a C_{60} construct would, for example, involve either bisetherification of protocatechuic aldehyde (3,4-dihydroxybenzaldehyde) with diethylene glycol under Mitsunobu type reaction conditions, or require attachment of diethanolamine unit in the hydroxyl function of isovanillin through a suitable linker. However, preliminary experiments along the former reaction failed to produce satisfactory yields of the anticipated diol. On the other hand, the construct obtained through the Prato reaction of C_{60} with a diethanolamine-modified isovanillin and Gly derivative **15**, after being pegylated, also failed to produce the anticipated bicarbonate 'active' ester with 4-nitrophenyl chloroformate in a satisfactory yield. We therefore decided to attach the preformed bicarbonate 'active' ester of a relatively simple diethanolamine derivative on a pegylated C_{60} construct using click chemistry (19). Accordingly, bromotoluic acid **22** was first converted to the corresponding azido derivative **23** in 88% yield, and the latter was coupled with diethanolamine, in the presence of HBTU, to produce the anticipated amide **24** (Scheme 3) in 77% yield. This compound was then unexceptionally activated with excess amount of 4-nitrophenyl chloroformate to produce the bisactivated intermediate **25** in 61% yield.

Nevertheless, alkylation of isovanillin with propargyl chloride gave compound **12** (Scheme 1) in 74% yield, incorporating a terminal alkyne unit. Prato reaction of C_{60} with aldehyde

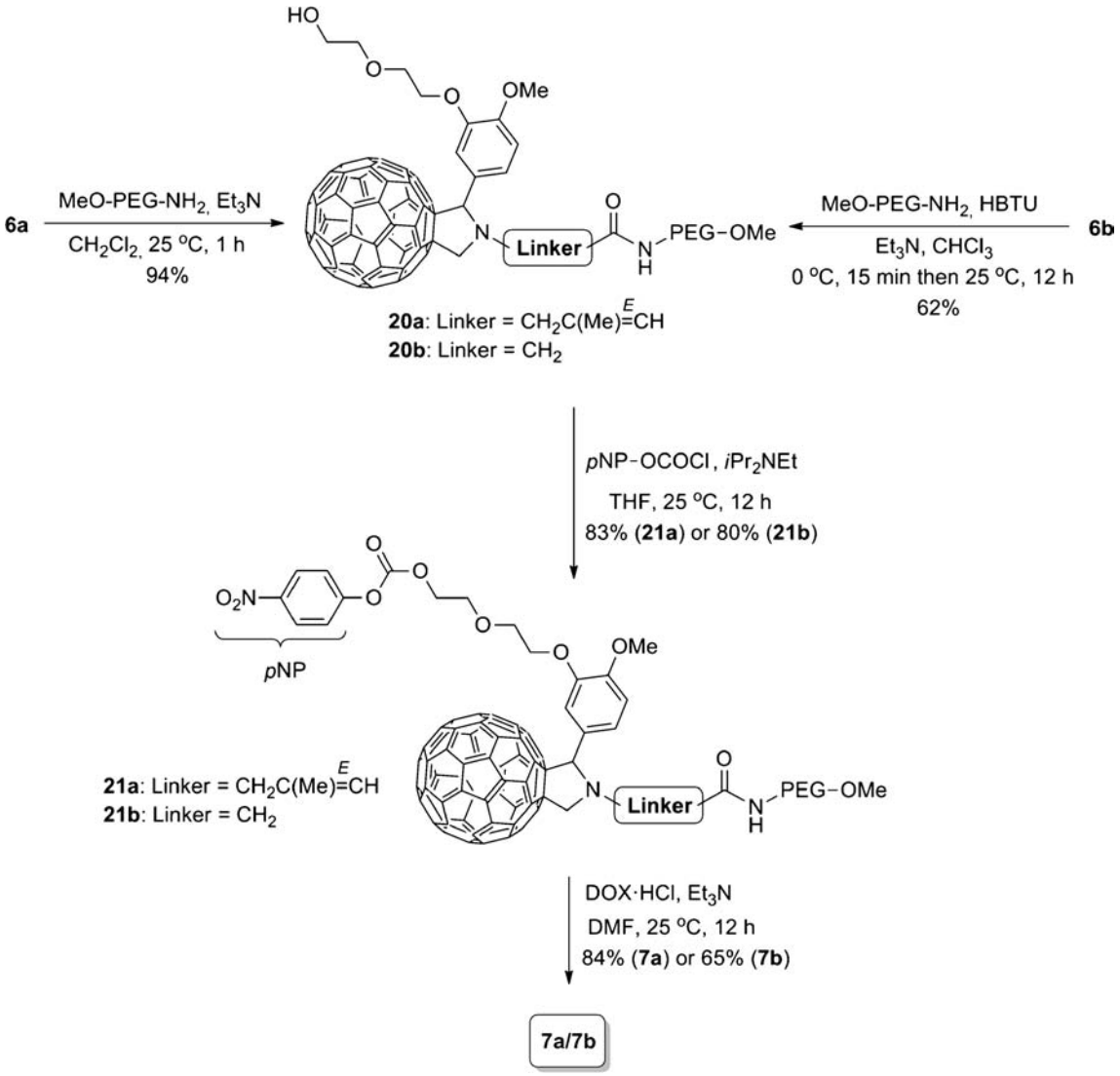

Scheme 2 Synthesis of the pegylated fullerene-doxorubicin conjugates **7a** and **7b**.

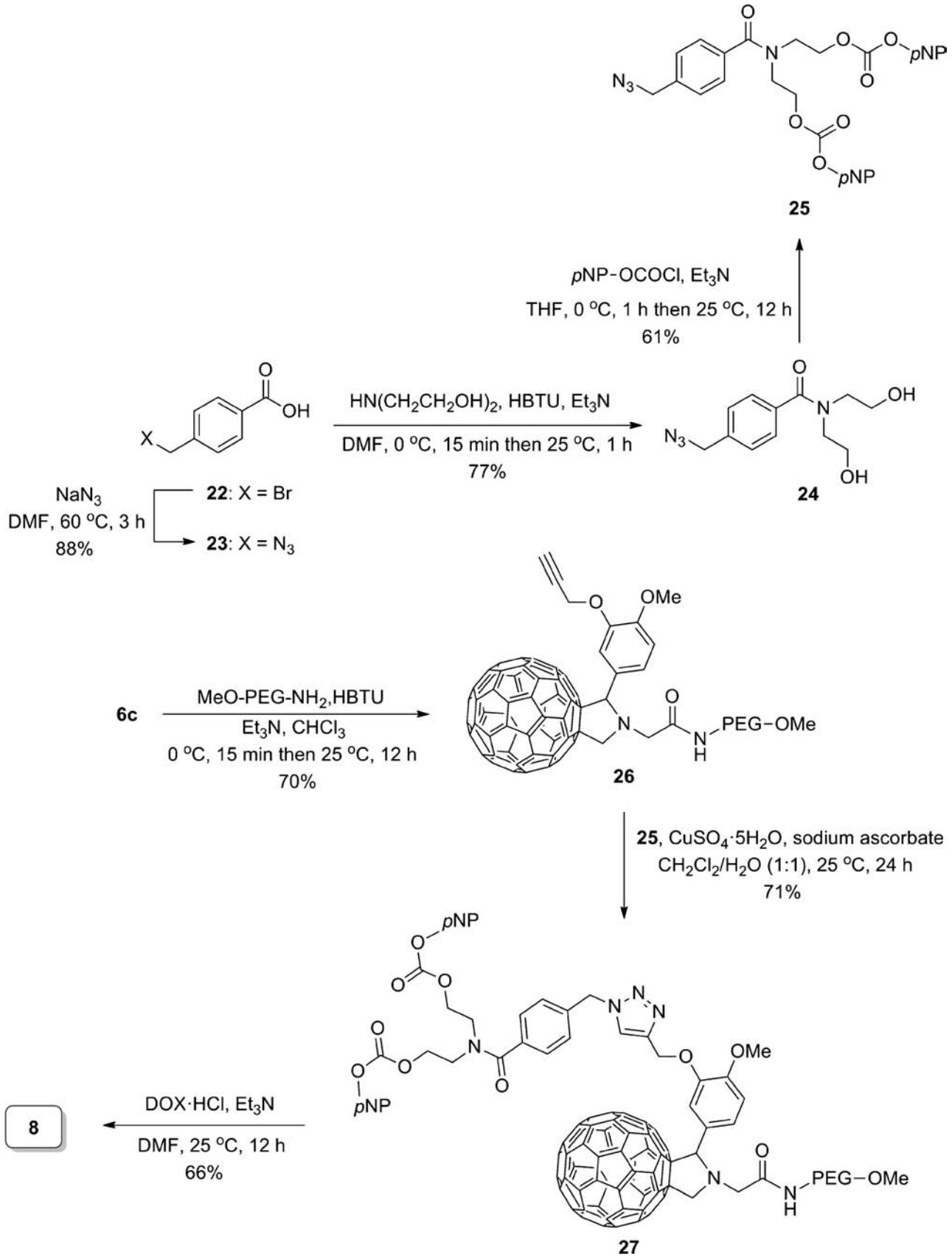

Scheme 3 Synthesis of the pegylated fullerene-doxorubicin conjugate **8**.

12 and Gly derivative **15** produced the fullerene adduct **19** (Scheme 1) in 44% yield. From this compound, the projected key-intermediate **6c** was obtained in 97% yield through CF_3CO_2H-mediated *tert*-butyl ester deprotection. Acid **6c** was then coupled with MeO- PEG-NH_2, in the presence of HBTU, giving rise to the pegylated C_{60} construct **26** (Scheme 3) in 70% yield. Click reaction between azide **25** and the terminal alkyne **26**, in the presence of $CuSO_4 \cdot 5H_2O$ and sodium ascorbate, proceeded unexceptionally to produce construct **27** in 71% yield. From this compound, the projected pegylated conjugate **8**, incorporating two DOX units, was obtained in 60% yield through aminolysis with DOX in the presence of Et_3N.

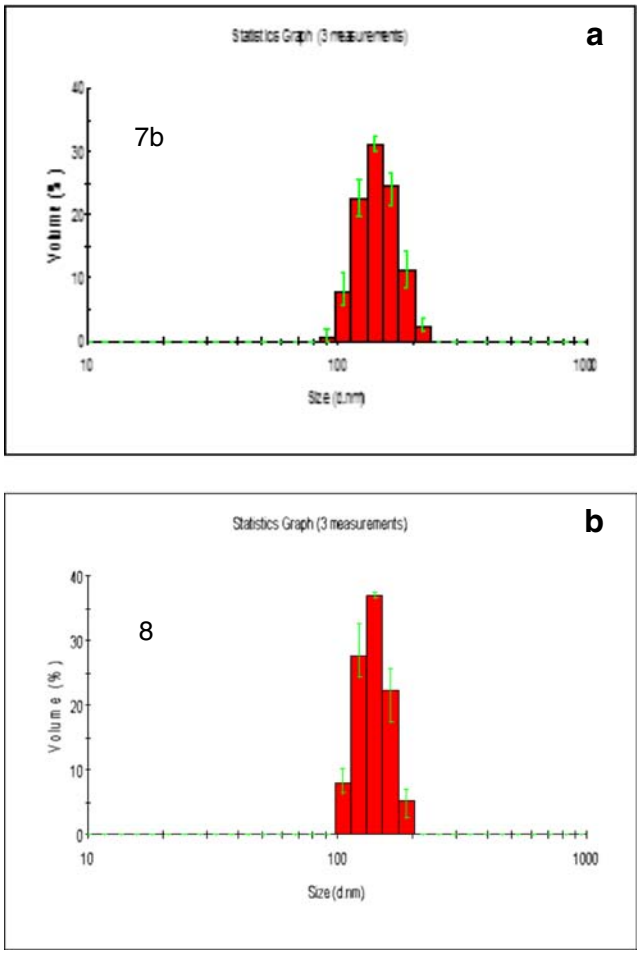

Fig. 2 Particle size distributions for DOX-C_{60}-PEG conjugates **7b** (**a**) and **8** (**b**) and DOX liberation from C_{60} particles (conjugate **8**) in PBS and MCF-7 cells lysate (**c**).

Physicochemical Characterizations and DOX Release from the Conjugates

We have found that the solubility of conjugate **7b** in water was 0.064% (*w*/*v*) or 180 μM . On the other hand, the solubility of

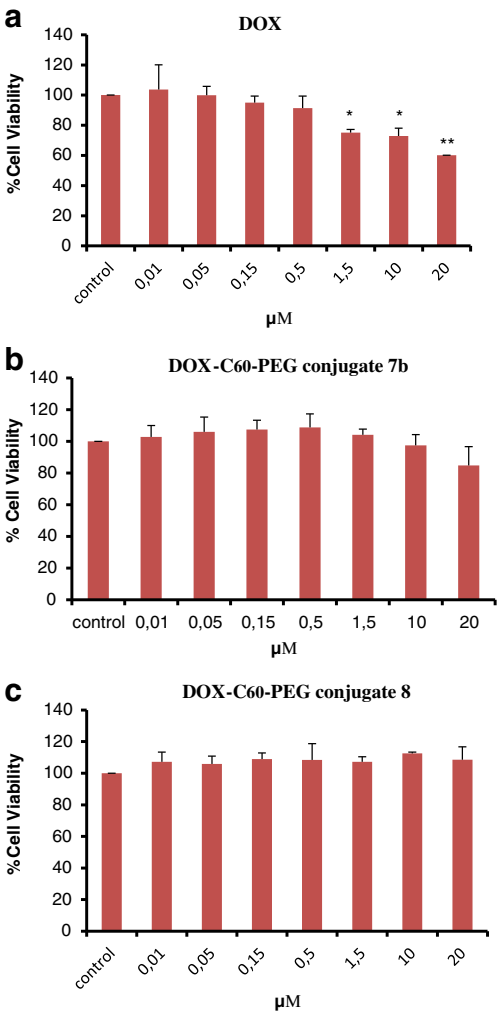

Fig. 3 Effects of DOX (**a**), DOX-C_{60}-PEG conjugate **7b** (**b**) and DOX-C_{60}-PEG conjugate **8** (**c**) on MCF-7 cells proliferation for a 24 h incubation period. A range of concentrations from 0.01 to 20 μM was assayed. The results are expressed as mean ± SD of three separate experiments in triplicate. Statistically significant differences were evaluated using the ANOVA test. Statistically significant differences among the treated and control cells are shown by (*) ($p \leq 0.05$) and (**) ($p \leq 0.01$).

conjugate **8** in water was 0.036% (*w*/*v*) or 83 μM. These results indicate that the pegylation with one PEG molecule of fullerene particle greatly enhanced its solubility in water, as pristine fullerene C_{60} is insoluble in water (its solubility in water has been estimated to be 1.3×10^{-11} mg/ml (20)). It appears also that the conjugate **7b** with one DOX molecule per fullerene particle is significantly more soluble in water than conjugate **8** with two DOX molecules. We have also found that fullerene compound **26**, intermediate in the synthesis **of 8**, was insoluble in water. However, the pegylated compound **26**, i.e. intermediate **6c**, was readily dissolved in water at ambient temperature without sonication. Information on the solubility of compounds **6c** and 2**6**, as well as of a non-pegylated fullerene-DOX conjugate, may be found in the Supporting Information.

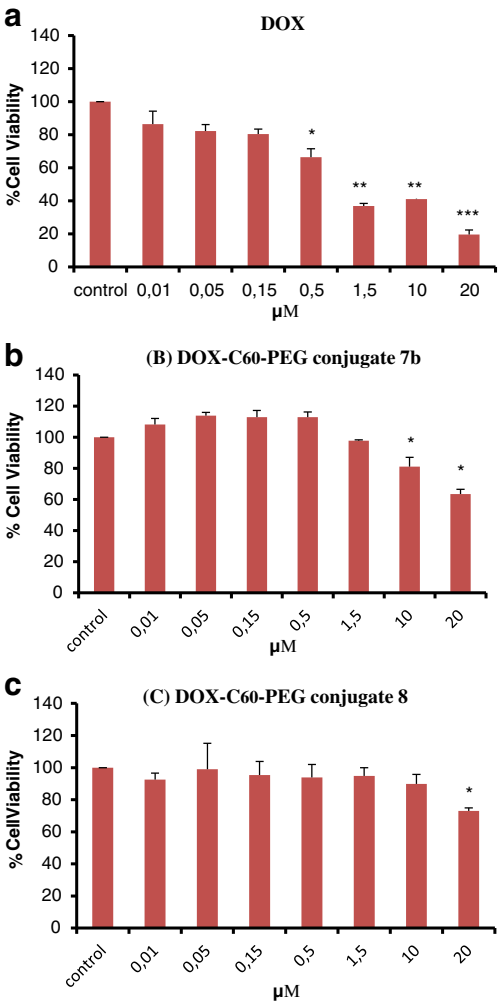

Fig. 4 Effects of DOX (**a**), DOX-C_{60}-PEG conjugate **7b** (**b**), and DOX-C_{60}-PEG conjugate **8** (**c**) on MCF-7 cells proliferation for a 48 h incubation period. A range of concentrations from 0.01 μM to 20 μM was assayed. The results are expressed as mean ± SD of three separate experiments in triplicate. Statistically significant differences were evaluated using the ANOVA test. Statistically significant differences among the treated and control cells are shown by (*) ($p \le 0.05$), (**) ($p \le 0.01$) and (***) ($p \le 0.001$).

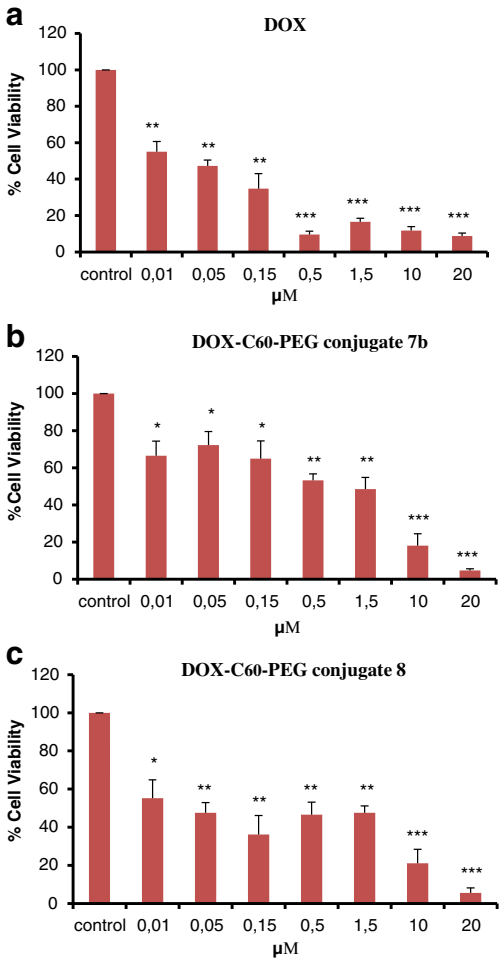

Fig. 5 Effects of DOX (**a**), DOX-C_{60}-PEG conjugate **7b** (**b**), and DOX-C_{60}-PEG conjugate **8** (**c**) on MCF-7 cells proliferation for a 72 h incubation period. A range of concentrations from 0.01 μM to 20 μM was assayed. The results are expressed as mean ± SD of three separate experiments in triplicate. Statistically significant differences were evaluated using the ANOVA test. Statistically significant differences among the treated and control cells are shown by (*) ($p \le 0.05$), (**) ($p \le 0.01$) and (***) ($p \le 0.001$).

Chaudhuri *et al.* (8) reported that PEG-Fullerenol-DOX conjugates form aggregates with an average size of around 80 nm whereas the anticipated particle size would have been expected to be no greater than 5 nm. The authors therein propose aggregation through molecular interactions, such as H bonding to explain this finding. We measured the particle size of conjugates **7b** and **8** (with one or two DOX molecules

Table I IC_{50} Values (μM) for Free DOX and DOX Conjugates at 48 and 72 h Incubation with the MCF-7 Cells

Compound	48 h	72 h
DOX	1.25	0.15
DOX-C_{60}-PEG Conjugate **7b**	51.46	18.23
DOX-C_{60}-PEG Conjugate **8**	24.18	11.23

per fullerene particle, respectively) in water using dynamic light scattering (DLS). The results obtained (Fig. 2a, b) indicate that the conjugates **7b** and **8** form aggregates with average sizes of 143 and 147 nm, respectively. These aggregates may form through hydrogen bonding. Indeed, DOX has several sites for donating or accepting H in hydrogen bonding-type interactions whereas the polymer chain (PEG-chain) has many sites (ether oxygen atoms) for acting as acceptors for hydrogen bonding. Intermolecular π-π interactions between aromatic regions of our PEG-C60-DOX conjugates might also add to the stabilization of such aggregates. DOX moieties, which incorporate two electron-rich rings and one electron-deficient (p-benzoquinone ring) might also offer possibilities for charge-transfer complex formation between conjugates leading to or enforcing aggregation.

In order to obtain evidence that the drug can be liberated from the fullerene particles intracellularly by enzymatic hydrolysis, conjugate **8** was incubated in MCF-7 cell lysate or PBS (pH 7.4). DOX was liberated slowly from the conjugate in cell lysate over one week, whereas comparatively little release of DOX occurred in PBS over the same time (Fig. 2c), suggesting that enzymatic processing would be important regarding the rate of drug liberation from the fullerene particles intracellularly. With regard to the slow release of DOX from conjugate even in PBS environment, our findings are in accordance with literature data for Fullerenol-DOX conjugates (8), in which conjugation is effected through the same type of bond, that is an urethane type bond. Although such a bond would be expected to be hydrolytically stable at pH 7.4, its slow hydrolysis in the phosphate buffer observed (Fig. 2c) might be attributed to the presence of the adjacent

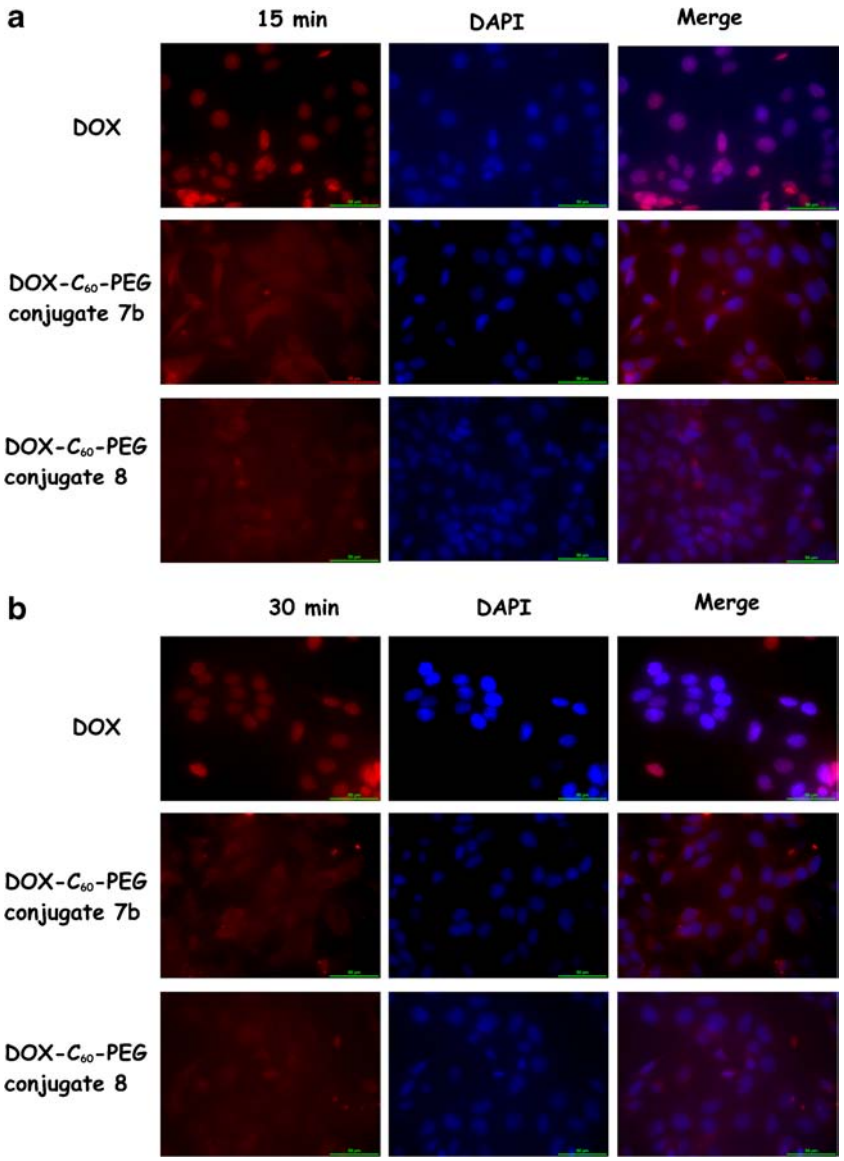

Fig. 6 Fluorescence imaging of DOX, DOX-C_{60}-PEG conjugate **8** and DOX-C_{60}-PEG conjugate **7b** after 15 and 30 min of incubation at 10 μM concentration. (**a**), 15 min - DOX is localized in the nucleus whereas the two conjugates appeared to be diffused in the cytoplasm. (**b**), 30 min - DOX remains in the nucleus. Conjugate 8 exhibit a perinuclear localization pattern, whereas conjugate **7b** diffused in the cytoplasm.

hydroxyl function which could act intramolecularly to catalyze the hydrolysis of the CO-NH bond.

Antiproliferative Activity

The inhibition of MCF-7 cells proliferation following incubation with free DOX and DOX-C_{60}-PEG conjugates **7b** and **8** for different time is shown in Figs. 3, 4, and 5. The antiproliferative effect of free DOX became significant at concentrations higher than 0.5 μM from the first 24 h of incubation, whereas the two DOX-C_{60}-PEG conjugates started to exhibit significant antiproliferative effect at concentrations equal or higher than 10 μM after 48 h of incubation. The conjugates exhibited high antiproliferative activity only after an incubation period of 72 h. At the 24 h incubation period, the IC_{50} values of free DOX and DOX conjugates were higher than 20 μM (Figs. 3, 4, and 5), the highest DOX concentration tested. The IC_{50} values for free DOX and DOX conjugates for 48 and 72 h incubation times were estimated using Graph Pad Prism 6.0 and are presented in Table I. Free DOX exhibited a trend for lower IC_{50} values compared to DOX conjugates. DOX-C_{60}-PEG conjugate **8** appeared to be more active than conjugate **7b**.

Cellular Uptake

The images of cells obtained with the fluorescent microscope (Figs. 6, 7, and 8) indicate that after 15 min free DOX was already accumulated in the cell nucleus (Fig. 6) where it is retained until 24 h of incubation (Fig. 6). After 24 h, no image could be obtained, since all cells were eliminated by apoptosis due to the action of DOX. Howbeit, after 15 min of

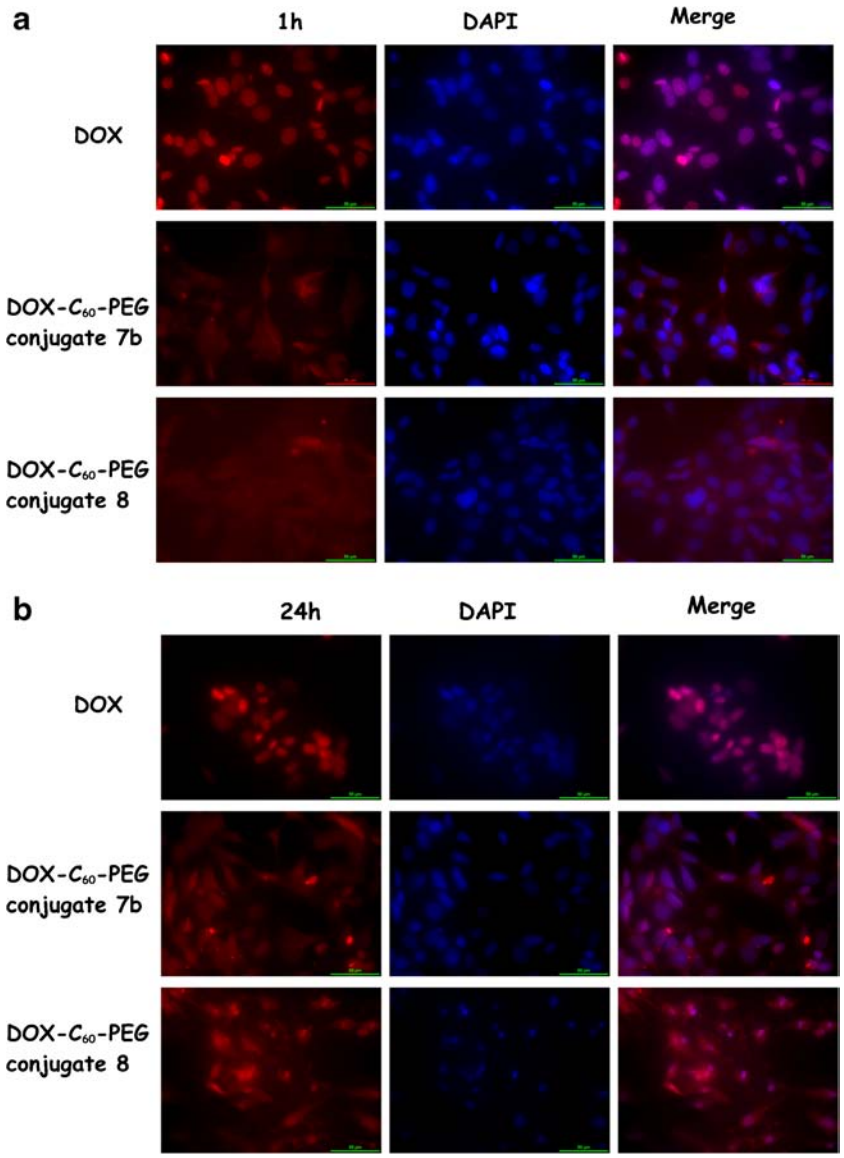

Fig. 7 Fluorescence imaging of DOX, DOX-C_{60}-PEG conjugate **7b** and DOX-C_{60}-PEG conjugate **8** following 1 and 24 h incubations at 10 μM concentration. (**a**), 1 h – DOX remains in the nucleus. Conjugate **8** exhibits a perinuclear localization pattern, whereas conjugate **7b** diffused in the cytoplasm (**b**), 24 h - DOX is still retained in the nucleus. The two conjugates are distributed mainly in the cytoplasm and there is evidence of them entering the nucleus.

incubation of the cells with conjugate **7b** or **8**, DOX started to be diffused in the cytoplasm and especially in the case of compound **7b** DOX seemed to be equally accumulated in the cytoplasm (Fig. 6). After 30 min, DOX from conjugate **7b** was more localized at the perinuclear region and its pattern became more clear, whereas the localization of DOX from conjugate **8** in the cytoplasm was slightly increased. Moreover, after 1 h the pattern of all compounds remained exactly the same (Fig. 7). After 24 h, free DOX was retained in the nucleus and apoptosis was obviously in progress since all cells nuclei appeared in the most characteristic state of programmed cell death shrunk, condensed and fragmented. Additionally, after 24 h of incubation of cells with conjugate **7b** or **8**, DOX was evenly distributed in the cytoplasm and there was also evidence of DOX entering the nucleus (Fig. 7). Finally, after 48 h of incubation of cells with conjugate **7b** or **8**, DOX entered the nucleus, the number of cells was decreased and apoptosis was established (Fig. 8). After quantification of the total fluorescence, it was found that as the time of incubation increases the amount of free DOX in the cell was gradually decreased, depicting its action in short time intervals (Fig. 9a). On the contrary, in the case of both DOX-C_{60}-PEG conjugates, the amount of DOX (free or still conjugated) revealed a peak of accumulation within the cell upon the incubation intervals 1 and 24 h for DOX-C_{60}-PEG conjugate 7b and 8, respectively (Fig. 9b, c). Thus, DOX conjugates contribute in the delayed internalization-localization within the cell and at second stage in the nucleus compared to free drug.

DISCUSSION

Water-soluble fullerene derivatives were recently shown to be capable of crossing cell membranes (21) and this opened the way for their potential application in drug delivery. As drug delivery vehicles, fullerene particles can provide several advantages, notably the feasibility of their functionalization which allows for drug, solubilizing and biofooling moieties to be attached on their surface, and the small particle size which would allow for targeting the conjugated on the fullerene particle drug molecule(s) to body sites with leaky vasculature, such as tumors and inflammation sites (22,23). In this work, we decided to take advantage of these desired properties of fullerenes as drug delivery vehicles for a more-specific (targeted) delivery of the potent anticancer agent doxorubicin through drug conjugation to fullerene particles.

Although a multiple decoration of C_{60} with anticancer drug units and other moieties necessary for efficient drug delivery could be potentially envisaged through a double functionalization of C_{60} using the Prato reaction, we preferred

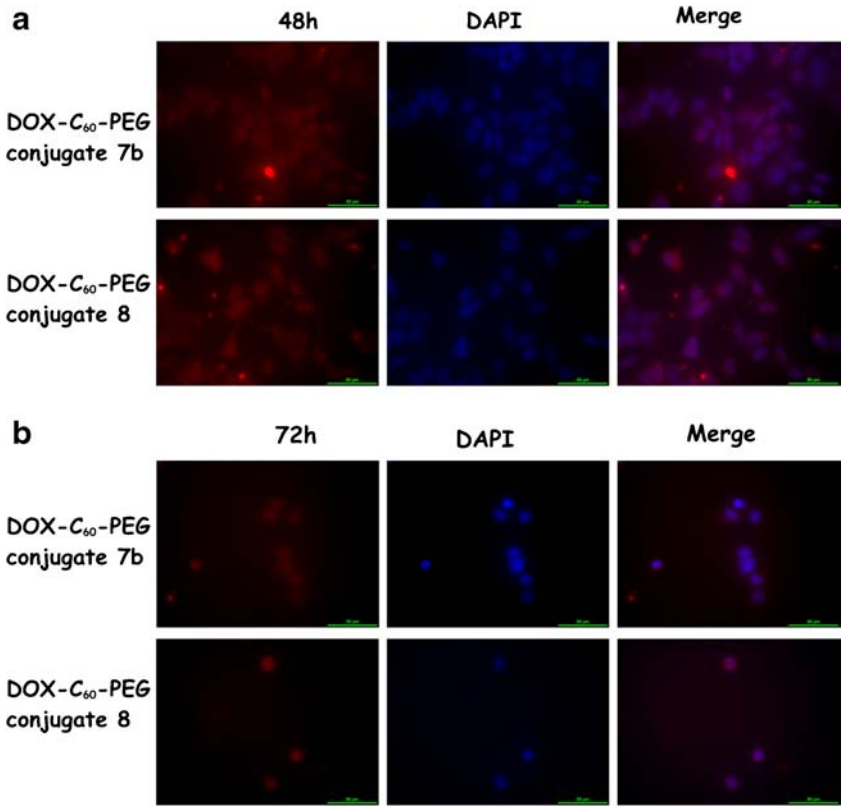

Fig. 8 Fluorescence imaging of DOX-C_{60}-PEG conjugate **7b** and DOX-C_{60}-PEG conjugate **8** after 48 and 72 h incubations at 10 μM concentration. (**a**), 48 h – and (**b**), 72 h – The conjugates are localized in the nucleus.

to create multiple arms on a monofulleropyrrolidine derivative, because a second Prato on a fulleropyrrolidine derivative is not as efficient as the first one and leads to a series of isomers (24). Based on our previous experience on attaching drug units on a polyamine functionalized fullerene we developed two alternative fullerenopyrrolidine constructs **6a** and **6b** which enabled us to load C_{60} with one molecule of DOX and one molecule of a water enhancing solubility PEG unit. Although **6a** coupled more efficiently with MeO-PEG-NH_2, **6b** was finally chosen as key-intermediate due to the shorter, more efficient and more cost effective synthesis of the N-alkylated Gly derivative required for the Prato reaction. Accordingly, the synthesis of the projected pegylated DOX-C_{60} conjugate **7b** was realized in three steps from fullerenopyrrolidine acid **6b** with 32% overall yield. On the other hand, for the successful loading of two DOX units on C_{60}, a different route was chosen. This included the click reaction between azide **25**, bearing two already activated hydroxyl functions and the terminal alkyne-functionalized fullerenopyrrolidine **26**, followed by aminolysis of the thus obtained construct **27** with DOX. Thus, the projected pegylated DOX-C_{60} conjugate **8** was obtained in 33% overall yield from the alternative fullerenopyrrolidine acid **6c**. The presence of one and two DOX moieties per C_{60} molecule in conjugates 7**b** and **8** respectively, was established through UV–vis studies (see supporting information). Further evidence for the increased loading of DOX in conjugate **8**, compared to conjugate **7b**, came from thermogravimetric analysis of the two conjugates. Interestingly, ^{1}H-NMR spectra of the aforementioned conjugates and conjugate **7a** also provided strong evidence that conjugate **8** incorporates two DOX units compared to conjugates 7**a** and 7**b**, which both contain one DOX unit (see supporting information).

Biological Evaluation

Free DOX exhibited significant antiproliferative activity on MCF-7 cells already from the first 24 h of incubation with the cells, whereas DOX conjugated to C_{60} had a significant, comparable to free DOX at relatively high doses, effect only after an incubation period of 72 h (Figs. 3, 4, and 5). It would appear that the antiproliferative effect develops more slowly in the case of conjugates than with the free drug, probably because, after conjugate entrance into the cells, the drug must be liberated from the conjugate in order to become active. Apparently, as the drug liberation in the presence of cell lysate suggests (Fig. 2), this process needs time. Pegylated fullerenol-DOX conjugates have been shown to be localized in the lysosomal compartment of the cell soon after cell entrance, where drug liberation from the conjugates can take place (8), and it is reasonable to assume a similar behavior for the conjugates synthesized in the present work. In accordance with the relatively slow effect of DOX-C_{60}-PEG conjugates on cells viability, DOX localization studies using fluorescence microscopy indicated that the drug is much more slowly localized in cell nucleus, where the drug can exert its pharmacological action, in the case of conjugates compared to free DOX (Figs. 6, 7, and 8). This assumption is further enhanced by the total fluorescence measurements (Fig. 9) where DOX conjugates revealed high accumulation of DOX within the cells at higher incubation times in comparison with free DOX. Microscopy images bear also witness of drug activity, as the number of cells is significantly reduced and nuclei of cells appeared in characteristic apoptotic state after 24 h of

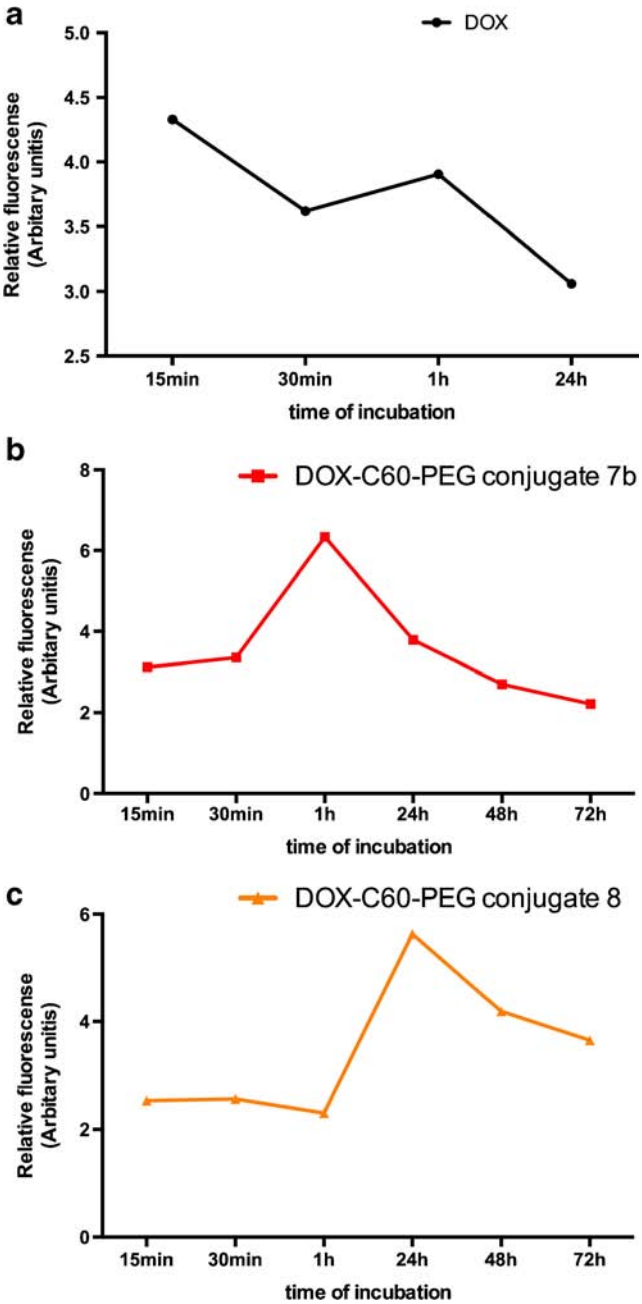

Fig. 9 Total DOX fluorescence within cells *versus* incubation time for free DOX (**a**), DOX-C_{60}-PEG conjugate **7b** (**b**) and DOX-C_{60}-PEG conjugate **8** (**c**).

incubation and later with the free DOX and after 72 h with the two DOX-C_{60}-PEG conjugates.

Both pure C_{60} and functionalized C_{60} exert oxidative stress–mediated photodynamic cytotoxicity (25,26). However, it appears that most of the pristine and functionalized fullerene preparations are not overtly toxic unless photoexcited or used at very high concentrations that are unlikely to be encountered during therapy (27). The blank (non- loaded with DOX) pegylated C_{60} particles (compound **26**, Scheme 3) exhibited antiproliferative effect only after prolonged (72 h) incubation with the cells at relatively high concentrations (Figure S4, supporting information). This antiproliferative activity of the blank pegylated C_{60} particles may be related to autophagy induction, a common cellular response to nanoparticles uptake (28), and does not represent a serious obstacle with regard to their application as anticancer drug carriers in cancer treatment, provided that, due to the EPR effect (22,23), they will accumulate preferentially at the tumor site.

CONCLUSION

One or two DOX molecules were successfully conjugated through biodegradable urethane bonds on pegylated fullerene particles to form stoichiometrically and structurally well-defined DOX-C_{60}-PEG conjugates. These conjugates exhibited comparable, but with a much more delayed onset, antiproliferative effect compared to free (non-conjugated) DOX when incubated with MCF-7 cells. Further studies towards uncovering the actual mechanism(s) through which these constructs exert their antiproliferative effect as well as the development of conjugates incorporating cancer cell targeting moieties and other, mechanistically differently acting, anticancer compounds are currently in progress.

ACKNOWLEDGMENTS AND DISCLOSURES

We wish to thank Dr. N. Eilert, University of Leipsig, for guidance regarding the preliminary biological results, Dr. G. Tsivgoulis, and Dr. K. Andriopoulou, Department of Chemistry, University of Patras, for UV/vis spectra and TGA measurements and related comments, respectively.

REFERENCES

1. Kroto HW, Heath JR, O'Brien SC, Curl RF, Smalley RE. C_{60}: Buckminsterfullerene. Nature. 1985;318:162–3.
2. Bosi S, Da Ros T, Spalluto G, Prato M. Fullerene derivatives: an attractive tool for biological applications. Eur J Med Chem. 2003;38(11–12):913–23.
3. Nakamura E, Isobe H. Functionalized fullerenes in water. The first 10 years of their chemistry, biology, and nanoscience. Acc Chem Res. 2003;36(11):807–15.
4. Hosseini A, Sharifzadeh M, Rezayat SM, Hassanzadeh G, Hassani S, Baeeri M, *et al.* Benefit of magnesium-25 carrying porphyrin-fullerene nanoparticles in experimental diabetic neuropathy. Int J Nanomedicine. 2010;5:517–23.
5. Shultz MD, Wilson JD, Fuller CE, Zhang J, Dorn HC, Fatouros PP. Metallofullerene-based nanoplatform for brain tumor brachytherapy and longitudinal imaging in a murine orthotopic xenograft model. Radiology. 2011;261(1):136–43.
6. Isobe H, Nakanishi W, Tomita N, Inno S, Okayama H, Nakamura E. Nonviral gene delivery by tetraamino fullerene. Mol Pharm. 2006;3(2):124–34.
7. Fillmore HL, Shultz MD, Henderson SC, Cooper P, Broaddus WC, Chen ZJ, *et al.* Conjugation of functionalized gadolinium metallofullerenes with IL-13 peptides for targeting and imaging glial tumors. Nanomedicine. 2011;6(3):449–58.
8. Chaudhuri P, Paraskar A, Soni S, Mashelkar RA, Sengupta S. Fullerenol-cytotoxic conjugates for cancer chemotherapy. ACS Nano. 2009;3(9):2505–14.
9. Lu F, Haque SA, Yang S-T, Luo PG, Gu L, Kitaygorodskiy A, *et al.* Aqueous compatible fullerene-doxorubicin conjugates. J Phys Chem C. 2009;113(41):17768–73.
10. Liu J-H, Cao L, Luo PG, Yang S-T, Lu F, Wang H, *et al.* Fullerene-conjugated doxorubicin in cells. ACS Appl Mater Interf. 2010;2(5):1384–9.
11. Zakharian TY, Seryshev A, Sitharaman B, Gilbert BE, Knight V, Wilson LJ. A Fullerene − paclitaxel chemotherapeutic: synthesis, characterization, and study of biological activity in tissue culture. J Am Chem Soc. 2005;127(36):12508–9.
12. Partha R, Mitchell LR, Lyon JR, Joshi PP, Conyers JL. Buckysomes: fullerene-based nanocarriers for hydrophobic molecule delivery. ACS Nano. 2008;2(9):1950–8.
13. Hirsch A, Brettreich M. In Fullerenes: Chemistry and Reactions. Weinheim: Wiley VCH; 2005.
14. WST-1 proliferation assay at http://lifescience.roche.com/shop/products/cell-proliferation-reagent-wst-1.
15. Burgess A, Vigneron S, Brioudes E, Labbé J-C, Lorca T, Castro A. Loss of human greatwall results in G2 arrest and multiple mitotic defects due to deregulation of the cyclin B-Cdc2/PP2A balance. Proc Natl Acad Sci U S A. 2010;107:12564–9.
16. Gavet O, Pines J. Progressive activation of CyclinB1-Cdk1 coordinates entry to mitosis. Dev Cell. 2010;18:533–43.
17. Potapova TA, Sivakumar S, Flynn JN, Li R, Gorbsky GJ. Mitotic progression becomes irreversible in prometaphase and collapses when Wee1 and Cdc25 are inhibited. Mol Biol Cell. 2011;22:1191–206.
18. Magoulas GE, Garnelis T, Athanassopoulos CM, Papaioannou D, Mattheolabakis G, Avgoustakis K, *et al.* Synthesis and antioxidative/anti-inflammatory activity of novel fullerene-polyamine conjugates. Tetrahedron. 2012;68(35):7041–9.
19. Iehl J, Pereira de Freitas R, Nierengarten J-F. Click chemistry with fullerene derivatives. Tetrahedron Lett. 2008;49(25):4063–6.
20. Heymann D. Solubility of fullerenes C60 and C70 in water. Lunar and Planetary Science. 1996;27:543–4.
21. Foley S, Crowley C, Smaihi M, Bonfils C, Erlanger BF, Seta P, *et al.* Cellular localization of a water-soluble fullerene derivative. Biochem Biophys Res Commun. 2002;294(1):116–9.
22. Moghimi SM, Hunter AC, Murray JC. Long-circulating and target-specific nanoparticles: theory to practice. Pharm Rev. 2001;53(2):283–318.
23. Maeda H, Wu J, Sawa T, Matsumura Y, Hori K. Tumor vascular permeability and the EPR effect in macromolecular therapeutics: a review. J Control Release. 2000;65(1–2):271–84.

24. Milic D, Prato M. Fullerene unsymmetrical bis-adducts as models for novel peptidomimetics. Eur J Org Chem. 2010;3:476–83.
25. Vileno B, Marcoux PR, Lekka M, Sienkiewicz A, Feher I, Forro L. Spectroscopic and photophysical properties of a highly derivatized C_{60} fullerol. Adv Funct Mater. 2006;16(1):120–8.
26. Markovic Z, Todorovic-Markovic B, Kleut D, Nikolic N, Vranjes-Djuric S, Misirkic M, *et al.* The mechanism of cell-damaging reactive oxygen generation by colloidal fullerenes. Biomaterials. 2007;28(36):5437–48.
27. Trpkovic A, Todorovic-Markovic B, Trajkovic V. Toxicity of pristine versus functionalized fullerenes: mechanisms of cell damage and the role of oxidative stress. Arch Toxicol. 2012;86(12):1809–27.
28. Zabirnyk O, Yezhelyev M, Seleverstov O. Nanoparticles as a novel class of autophagy activators. Autophagy. 2007;3(3):278–81.